[19] Balestrino, A., De Maria, G., Sciavicco, L., "Robust Control of Robotic Manipulators", Proc. 9th. IFAC World Congress, Budapest, Hungary, 1984.

[20] Wolovich, W.A., Elliott, H., "A Computational Technique for Inverse Kinematics", Proc. 23rd. Conf. on Decision and Control, Las Vegas, NV, Dec. 1984.

[21] Sciavicco, L., Siciliano, B., "A Solution Algorithm to the Inverse Kinematic Problem for Redundant Manipulator", IEEE Jour. of Robotics and Automation, Vol. 4, No. 4, Aug. 1988.

[22] Das, H., Slotine, J.J.E., Sheridan, T.B., "Inverse Kinematic Algorithms for Redundant Systems", Proc. IEEE Int. Conf. on Robotics and Automation, San Francisco, CA, 1988.

[23] Melchiorri, C., Salisbury, J.K., "Exploiting the redundancy of a hand/arm robotic system", A.I. Memo No. 1261, Artificial Intelligence Laboratory, MIT, Cambridge, MA, Oct. 1990.

Experimental Evaluation of Friction Characteristics With an Articulated Robotic Hand

Antonio Bicchi *
J. Kenneth Salisbury †
David L. Brock ‡

Massachusetts Institute of Technology
Artificial Intelligence Laboratory

Abstract

In this paper some applications of dexterous robotic hands to fine manipulation operations are discussed. Common to this kind of operations is the important role played by the frictional characteristics of the fingers and of manipulated objects. The paper discusses a procedure for measuring apparent coefficients of friction between the fingertips and manipulated objects. To take into account real contact phenomena, the distinction is introduced between translational and rotational friction limits. Reported experiments rely on force-based (intrinsic) contact sensing devices, implemented in the phalanges of an articulated robot hand (Salisbury Hand). Data collected during these procedures can be subsequently used for tasks such as recognizing the superficial features of objects, controlling the internal grasp forces exerted by the hand on delicate objects, and following the contours of the surface of unknown objects.

1 Introduction

While robots seem to have saturated the easiest applications in the factory environment, a great potential remains for robots to be employed in unstructured surroundings and non conventional tasks. In order for a robot to prove useful in such conditions, however, a higher level of dexterity in its operations than is currently available has still to be achieved. Dexterous articulated hands have been proposed since the early '80 by several researchers, e.g. Mason and Salisbury [1], Jacobsen *et al.* [2]. However, full exploitation of their capabilities has not yet been accomplished, mainly because of the lack of adequate contact sensing technology. Conventional, "skin-like" tactile sensing devices in fact, though intriguing for their similarity to the biological model, failed so far to provide an accurate, reliable feedback of the interactions between the robot hand and grasped objects. These devices also suffer from some other drawbacks, such as limited resolution and/or bandwidth, encumbrance, large number of connectors. A detailed report on the state-of-the-art for conventional tactile sensors can be found in [3].

Probably, the most severe limitation of skin-like tactile sensors is that frictional forces transmitted through contact can not be satisfactorily sensed. Pioneering work in designing skin-like

*Antonio Bicchi is currently a Research Associate on leave from the Department of Electric Systems and Automation (DSEA) and Centro "E. Piaggio," Università di Pisa, Italia.

†J. Kenneth Salisbury is currently a Research Scientist at the Artificial Intelligence Laboratory at Massachusetts Institute of Technology.

‡David Brock is currently a Ph.D. candidate in the Department of Mechanical Engineering at Massachusetts Institute of Technology.

tactile sensors with the capability of discerning tangential stresses, such as that presented by Hackwood *et al* [4], and by Domenici *et al.* [5], has not till yet been applied to building practical devices. On the contrary, in some cases (e.g. for some piezoelectric film based sensors) friction forces produce aliasing in contact pressure measurements.

The fundamental role played by friction in the control of manipulation operations is apparent. Humans rely on friction forces in many of their grasping or manipulating operations: this is perhaps reflected in our uneasiness with slippery hands. Controlling the slippage of grasped objects, on the other hand, allows us to achieve high dexterity in object manipulation. In order to replicate at least part of the human manipulative capabilities, it is therefore necessary to be able to sense friction, and to control (to avoid, or, sometimes, to allow) slippage.

In the following, we will present some experiments intended to assess the feasibility of friction sensing with a non conventional contact sensing device, namely a force/torque based, or intrinsic, contact sensor. While the theory underlying this sensing principle is presented elsewhere [6], we show here that those sensors are well suited to deal with friction forces in fine manipulation operations, and can provide for a major advancement in the dexterity of robots.

2 Contact and Friction Model

An accurate model of the phenomenology related to contact is very difficult to describe. In fact, contact involves so many factors, both intrinsic to the touching bodies (such as their macro- and microscopic geometry and elastic properties), and extrinsic (lubrication, temperature etc.), that a comprehensive modelization is hopeless, except for very idealized cases. Research in the field of tribology has evidentiated the difficulty in providing a single model of friction valid over a broad range of circumstances. Armstrong [7] [8] provides a good reference and a vaste bibliography concerning tribologic problems relevant to robotic actuation and control. For our purposes here, however, so fine a physical description of contact phoenomena is not necessary. For instance, in many dextrous manipulation operations slippage is to be considered an undesirable loss of control to be avoided, so that we are primarily concerned with static friction limits. If a relative motion of the fingers on the object surface is desired (such is the case in the surface following task described by Balestrino and Bicchi [9], or in advanced dexterity operations as described by Brock [10]), it usually consists of a constant speed, quasi-static motion. In modeling the contact interaction between the end effector and the object surfaces, therefore, we will make some simplifying assumptions, such that an operative model of contact and friction results.

2.1 Contact Model and Contact Sensors

Consider the contact of two deformable bodies pressed against each other, as depicted in Fig. 1: we will refer to these bodies as to the *finger* and the *object*. The contact area will be in general composed of several non-connected small zones, distributed over the deformed surfaces in contact.

A force/torque based (intrinsic) contact sensor can be realized in the fingers of the robot hand by employing a six-axis force sensor to measure the resultant force and torque exerted on the finger surface through contact [6]. Since intrinsic contact sensors are instrumental in the manipulative operations that we are going to describe, the concepts underlying their functioning will be briefly recalled.

A *contact centroid* on a contact surface is defined as a point c such that there exists a force p through that point, and a moment q normal to the surface at that point, which form a set of forces equivalent to the actual contact load. It can be shown that, under certain commonly verified assumptions, the contact centroid enjoys the property of being unique, and lies inside

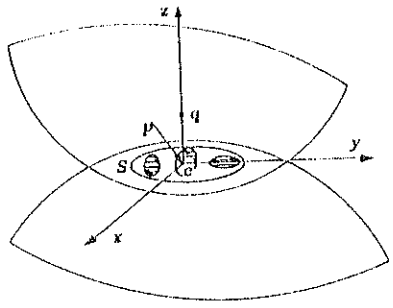

Figure 1: Soft-finger contact model

the convex hull S that encloses every contact zone. An intrinsic contact sensor is capable of providing the location of the contact centroid on the finger surface, along with the measurements of the components of the contact force and torque.

The above mentioned assumptions regard convexity and smoothness of the finger surface; it is also assumed that only compressive forces are exerted by contact (no adhesion). A further limitation applies to the allowable warping of the contact area over the contact surfaces; this bound can be quantitatively expressed in terms of the frictional properties of the surfaces and of their geometry. For a precise statement of these hypotheses, and for a proof of the contact centroid properties, the interested reader is referred to [6]. In the context of this paper, we will make a stronger assumption, i.e. that the contact area warping over the curved contacting surfaces is negligible altogether. This condition will be useful in modeling friction effects, and is satisfied in most practical circumstances of robotic manipulation.

Consider a cartesian reference frame with origin in the contact centroid c and z-axis aligned with the normal to the contacting surfaces. At each point $\mathbf{r} = (r_x, r_y)^T$ of the contact area, bodies mutually exert tractions $\mathbf{h}(\mathbf{r})$ whose normal component h_z is usually referred to as *pressure*, while h_x and h_y are friction components. With respect to that reference frame, the resultant contact force vector p is defined as

$$\mathbf{p} = \int_S \mathbf{h}(r)\, dS$$

while the components of the resultant torque vector q are given, by definition of contact centroid, by

$$\begin{aligned} q_x &= 0, \\ q_y &= 0, \\ q_z &= \int_S (h_y r_x - h_x r_y)\, dS. \end{aligned}$$

In order to control manipulation, we are interested in the physical constraints imposed on the components of p and q. The pressures on the object, and their resultant p_z, must be compressive and not larger than a limit value, which depends on the object and/or the finger

strength. The limit value for the allowable contact force is an important factor in the choice of the grasp forces. Since complex and not yet completely understood mechanics are involved in the resistance of materials to contact forces, we will adopt conservative bounds on $\mathbf{p}_c$ (or possibly on the intensity of the force contact vector $\mathbf{p}$). The remaining components of contact force and torque are generated by friction phenomena, and hence their limitations depend on the assumed friction model, briefly discussed in the following subsection.

2.2 Friction Model

In the following we will consider the classical, simplified model summarized as follows:

> the friction force exerted on a point lying on a surface with zero relative velocity is equal and opposite to the sum of external forces tending to move the point. The maximum force that can be sustained in this way by friction is proportional (by a static coefficient of friction μ_s) to the normal force pressing the point on the surface. If the object is moving with respect to the surface, the friction force opposes the relative velocity with an intensity proportional (by a kinetic coefficient of friction μ_d, generally lower than μ_s) to the normal force.

This model of friction is expressed by the relationship

$$\left.\begin{aligned} \mathrm{h}_x &= \mathrm{f}_x \\ \mathrm{h}_y &= \mathrm{f}_y \end{aligned}\right\} \qquad \begin{aligned} \mathbf{v} &= 0 \\ \sqrt{\mathrm{h}_x^2 + \mathrm{h}_y^2} &\leq \mu_s \mathrm{h}_z \end{aligned}$$

$$\left.\begin{aligned} \mathrm{h}_x &= -\frac{\mathbf{v}_x}{\|\mathbf{v}\|}\mathrm{h}_z\mu_d \\ \mathrm{h}_y &= -\frac{\mathbf{v}_y}{\|\mathbf{v}\|}\mathrm{h}_z\mu_d \end{aligned}\right\} \qquad \mathbf{v} \neq 0$$

where $\mathbf{v} = (\mathbf{v}_x, \mathbf{v}_y)^T$ is the velocity of the point relative to the surface in the contact plane (see Fig. 1), and f is the external solicitation on the contact. As it can be seen, possible dependencies of friction on slip rate or history are disregarded in this model, and a discontinuity in the friction force in corrispondence of a starting motion is admitted.

When a finite area of contact is considered, limitations on allowable friction forces are more involved. If we consider non rigid surfaces, in particular, we have that some points in the contact area may move, while others do not. Therefore, it is possible to have mixed static and kinetic friction effects. Moreover, even in the assumption that the contact area is and remains in the contact plane before and immediately after slippage, the combined effect of soliciting forces $\mathrm{f}_x, \mathrm{f}_y$ and torque t_z must be considered.

Consider first the case that a pure force f is applied to the bodies in contact at the contact centroid, and that the tangential component of f is gradually increased. At a certain instant (and in relation with the details of how f is transmitted to the contact interface), slippage will start at some contact points, where friction will abruptly drop to its kinetic value. A redistribution of the contact load then follows, and more points will be lead to slip. If the tangential component of f is increased enough, the slip 'wavefront' will sweep the whole contact area, and the two surfaces will start sliding on each other (this phenomenon, which has similarities with classical plasticity models, gives rise to acoustic waves propagating in the bodies, whose detection could be used as a means for detecting slippage [11]). Since the contact centroid, for planar contacts, coincides with the center of friction of the contact area [1], the act of relative motion immediately following is a translation. The maximum intensity of the tangential component of the contact force f that can be absorbed by friction in this case obeys the limitation

$$\sqrt{\mathrm{f}_x^2 + \mathrm{f}_y^2} \leq \int_S \mu(\mathbf{r})\, \mathrm{h}_z(\mathbf{r})\, dS. \tag{1}$$

where $\mu(\mathbf{r})$ equals either $\mu_s(\mathbf{r})$ or $\mu_d(\mathbf{r})$, depending upon the relative velocity $\mathbf{v}(\mathbf{r})$ at the contact area element dS. From an operative point of view this expression is impractical, and a more convenient expression can be obtained if we assume that an *equivalent* coefficient of friction μ_{eq} exists such that, at the instant when the last contact point starts slipping, we have

$$\sqrt{\mathrm{f}_x^2 + \mathrm{f}_y^2} = \mu_{eq}\mathrm{f}_z \tag{2}$$

Such relationship can also be interpreted as if all points in the area of contact were starting to slip at the same instant: the local static coefficient of friction is substituted everywhere by a lower value, μ_{eq}, to take into account the apparent decrement of friction due to partial slip.

Consider now the case that a purely normal contact force is exerted between the finger and the object, and that the torsion t_z is gradually increased, until slippage occurs at every contact point. By symmetry reasons, the instantaneous center of rotation (COR) of the motion immediately following the first occurrence of sliding coincides with the contact centroid, so that we can write the upper bound of friction torque as

$$\mathrm{t}_z \leq \int_S \mu(\mathbf{r})\, \mathrm{h}_z(\mathbf{r})\, \|\mathbf{r}\|\, dS. \tag{3}$$

The evaluation of eq. 3 is not simple in general. Jameson [12] assumes that the results of Hertzian theory concerning the normal pressure distribution and the contact area shape hold even in the presence of friction forces, and gives an expression for a spherical fingertip and object:

$$\mathrm{t}_z \leq 0.59\, \mu_{eq}\, \alpha^{1/3}\, \mathrm{f}_z^{4/3}, \tag{4}$$

where the equivalent friction coefficient μ_{eq} is introduced, as above, to take into account progressive slippage phenomena, and α is a constant depending upon geometric and elastic properties of the contacting bodies [12].

From eq. 4 a general proportionality relationship may be hypothesized for generic non-conformal surfaces pressed against each other by a normal contact force f_z:

$$\mathrm{t}_z \leq \nu_{eq}\, \mathrm{f}_z^{4/3}, \tag{5}$$

where ν_{eq} is a characteristic of the peculiar contact conditions. Note that the more-than-linear dependence of the maximum friction torque upon the contact force, may be interpreted as the result of the twofold effect of contact force, which increases local friction forces and enlarges the contact area (due to deformations of the bodies) as well.

If a torsion is applied at the contact along with tangential forces, the COR of slippage motion is not at the contact centroid, and therefore eq. (5) does not hold. The limits of friction resistance under combined shear and torsion loading have been studied by Jameson [12] and by Howe, Kao and Cutkosky [13], with reference to the case of contact between non-conformal (in particular, spherical) bodies. In this case, only the intensity of shear forces, $\mathrm{f}_t = \sqrt{\mathrm{f}_x^2 + \mathrm{f}_y^2}$ is of interest, due to the symmetry of the problem. In the cited papers, it is shown that slippage occurs for combined loadings whose representative points in a shear force - torsion plane lie outside a convex curve (see Fig. 2). The authors also show that, given the limit values of friction under pure shear force (eq. (2)) and under pure torsion (eq. (5)), an ellipse approximates well the limit curve, while a linear interpolation provides a conservative approximation of the actual friction limit curve.

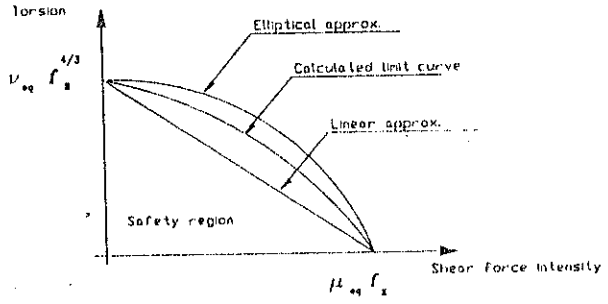

Figure 2: Sliding under combined torsion and shear loading for spherical surfaces (adapted from Howe, Kao and Cutkosky [12]

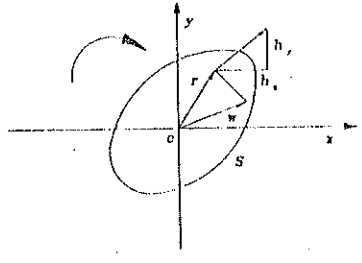

Figure 3: Sliding under combined torsion and shear loading for planar surfaces

The general case of contact between conformal surfaces (such as two portions of parallel planes, as occurs in grasping by parallel jaw grippers), is even more complex. With reference to Fig. 3, let the position of the COR in the contact centroid frame be the vector $\mathbf{w}$.

The maximum values that can be attained by friction forces and torque can be expressed in general as

$$|f_x| \leq \int_S \frac{\mathbf{r}_y - \mathbf{w}_y}{\|\mathbf{r} - \mathbf{w}\|} \mu(\mathbf{r})\, \mathbf{h}_z(\mathbf{r})\, dS, \tag{6}$$

$$|f_y| \leq \int_S \frac{\mathbf{r}_x - \mathbf{w}_x}{\|\mathbf{r} - \mathbf{w}\|} \mu(\mathbf{r})\, \mathbf{h}_z(\mathbf{r})\, dS, \tag{7}$$

$$|t_z| \leq \int_S \|\mathbf{r} - \mathbf{w}\| \mu(\mathbf{r})\, \mathbf{h}_z(\mathbf{r})\, dS + \mathbf{w}_x \mathbf{r}_y - \mathbf{w}_y \mathbf{r}_x. \tag{8}$$

In practice, the problem is posed in a different way: given the applied friction forces and torque (e.g. by means of intrinsic contact sensors: $\mathbf{p} = \mathbf{f}, \mathbf{q} = \mathbf{t}$), we wish to know how close the danger of slippage is. Since the COR position is not known a priori, we need to solve any two

of the three equations above for $\mathbf{r}$, and then obtain the bound on the third component of the frictional load. However, such solution requires both the knowledge of the contact area shape and of the pressure distribution over it, and can only be obtained numerically. References to this problem can be found in several authors' work, among which [1], [14], [13]; experimental results with an integrated (skin-like + intrinsic) tactile sensor have been described in [15].

3 Measurement of Friction Characteristics

As discussed above, it is rather difficult to predict, on theoretical grounds, the frictional characteristics of the contacts occurring in fine manipulation operations. On the other hand, such data are very important for the correct control of the robot hand. It is the authors' belief that, for most practical applications of robot hands, the evaluation of friction limits provided by the approximations described in Fig. 2 is sufficient to guarantee proper operation of the hand. To use those approximations (namely, the conservative linear approximation and the elliptical approximation), it is necessary to know the limit values of friction resistance in the cases of pure shear load and pure torsion. To this purpose, we devised a procedure for characterizing frictional effects by means of direct measurements in operative conditions, i.e. using exactly the same apparatus (hand, fingertips, objects) and in the same environmental conditions that are going to be met in the manipulative task.

3.1 Experimental Setup

The experiments described below have been carried out at the MIT AI Lab using contact sensors mounted on the distal phalanx of the fingers of the Salisbury articulated hand [1], fixed in turn to the wrist of a Unimation Puma manipulator. The low-level trajectory interpolation and control of the finger joints is performed by two 6-axis Unimation industrial controllers.

Part of the experiments have been carried out with a high-level control architecture consisting of a dedicated DEC VAX computer and a Lisp machine (see [16]), running the hand programming environment OOLAH [17]. Later on, the high-level control system architecture has been modified and consists now of three processors Motorola 68030 on a VME bus, working in the parallel-processing, real-time environment provided by the VxWorks operating system.

We employed joint position sensors (encoders located at the actuator shafts). The force based contact sensors described in [18] have been used interchangeably with those described in [19]. The rest of the sensory equipment of the Salisbury hand (tendon tension sensors, palm contact sensor, and others) have not been employed in the experiments described below.

3.2 Translational Friction Characteristics

In Fig. 4 a generic object is grasped by means of the fingers of a robot hand. The fingers are supposed to be equipped with contact sensors, providing measurements of contact forces and torques. The position of the fingers relative to the grasped object is supposed to be such that the resulting grasp is stable enough to be robust with respect to small perturbations of the location of the fingers. The procedure to obtain static and kinetic coefficients of friction relative to translational slippage (due to pure shear) of the i th finger on the grasped object surface is as follows:

- One of the fingers, e.g. the thumb, bearing the sensorized fingertip and opposing the other two fingers in the grasp, is imparted a time-increasing force in the contact plane, tending to move the finger along the object surface, while the normal component of the contact force is regulated at a constant value;

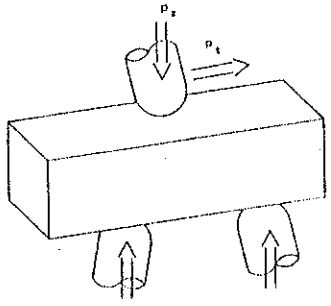

Figure 4: The robot hand fingertips and the object during the measurement of translational friction limits

- The starting motion of the finger is detected by joint position sensors, and the finger is stopped after a very short motion (1 mm);
- The force and torque transmitted by contact are measured by the fingertip sensor;
- The normal and tangential components of the contact force are computed by applying the intrinsic contact sensing algorithm to the force/torque data.

Finally, from observation of the time history of the friction ratio

$$R_f = \frac{p_x}{\sqrt{p_x^2 + p_y^2}},$$

the desired information on friction coefficients can be derived. A typical plot of the (adimensional) values of R_f vs. time (in tenths of a second) in the experiment above described is reported in Fig. 5 (data are relative to an urethane-steel contact).

Observing this and many other experimental diagrams, a common pattern could be recognized by sight, consisting of two separate parts: initially, there is an almost linear increase of the friction ratio up to a maximum value, then a more or less abrupt change to a lower value. The latter is subsequently held without significant variations. Such pattern is in good agreement with the expectations based on the simplified classical model of friction discussed in section 2: the friction ratio increases during phase 1, until it reaches the (apparent) static coefficient of friction, after which R_f drops to a value corresponding to kinetic conditions.

The desired friction coefficients, μ_s and μ_d, might be obtained by considering the n samples of the friction ratio, $R_f(i), i = 1, n$ corresponding to instants $t = iT$ (T is the sampling period), simply as

$$\mu_s = \max_{i=1,n}\{R_f(i)\}, \tag{9}$$

$$\mu_d = \frac{\sum_{i=s}^{n} R_f(i)}{n - s}. \tag{10}$$

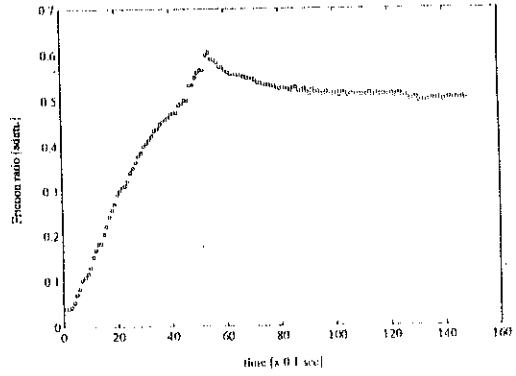

Figure 5: Friction ratio vs. time in a typical contact experiment between steel and urethane surfaces

where s is the sample corresponding to the maximum R_f, immediately preceding slippage. However, experimental tests repeatedly carried out on the same object in apparently similar conditions, showed that the estimates obtained through eq. (9) and eq. (10) are too sensitive to small perturbations of data, such as those due to sensor noise, vibrations of the robot structure, and in general to the poorly deterministic character of the complex phenomenon of friction.

To overcome this problem, a more robust algorithm has been devised, based on the idea of matching experimental data with the expected pattern of friction. The set of measurements $R_f(i)$ is split in two parts, preceding and following the k^{th} sample. A least-squares linear approximation of the subset of data preceding the k^{th} sample is evaluated as

$$\hat{R}_f(j) = a_k\, j + b_k, \tag{11}$$

$$a_k = \frac{k\sum_{j=1}^{k} j\, R_f(j) - \sum_{j=1}^{k} j \sum_{j=1}^{k} R_f(j)}{k\sum_{j=1}^{k} j^2 - (\sum_{j=1}^{k} j)^2}, \tag{12}$$

$$b_k = \frac{k\sum_{j=1}^{k} j^2 \sum_{j=1}^{k} R_f(j) - \sum_{j=1}^{k} j \sum_{j=1}^{k} j\, R_f(j)}{k\sum_{j=1}^{k} j^2 - (\sum_{j=1}^{k} j)^2}. \tag{13}$$

The remaining samples $R_f(i), k < i \leq n$ are approximated by a constant c_k equal to their mean value. The average quadratic errors corresponding to the approximations of the first and second data set are evaluated as

$$\sigma_1(k) = \frac{\sum_{j=1}^{k}(R_f(j) - a_k j - b_k)^2}{k}, \tag{14}$$

$$\sigma_2(k) = \frac{\sum_{j=k}^{n}(R_f(j) - c_k)^2}{k}, \tag{15}$$

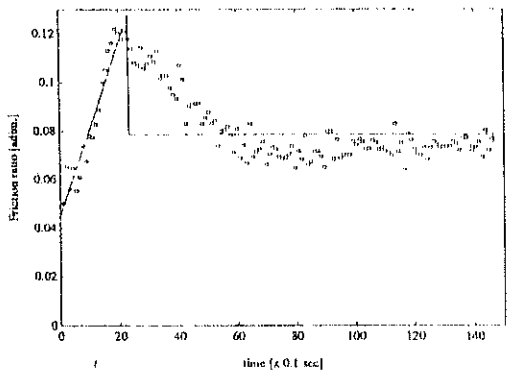

Figure 6: Friction ratio plot for an ABS plastic-steel pair

and their sum, $\sigma = \sigma 1 + \sigma 2$, is computed as k spans the time axis; the value $k = \hat{k}$ that minimizes $\sigma(k)$ is assumed to correspond with the beginning of slippage. Accordingly, the estimated friction coefficients are:

$$\mu_s = a_{\hat{k}}\hat{k} + b_{\hat{k}}, \tag{16}$$

$$\mu_d = c_{\hat{k}}, \tag{17}$$

while the sum of average quadratic errors $\sigma(\hat{k})$ is used as a measure of the dependability of these estimates.

The results of experimental tests carried out with three different pairs of finger and object cover materials are reported in Fig. 6, Fig. 7, and Fig. 8, respectively.

Superposed to the friction ratio measurements (small squares) are the lines corresponding to the approximating pattern above described. Particularly interesting is the plot of Fig. 8 (steel on a thickly painted wooden block), showing how the measured friction ratio bounces several times between the static and kinetic friction coefficient values before settling at the lower (kinetic) value. This phenomenon is due to stick-slip motion of the finger on the object surface (this irregular motion could be easily verified also by visual inspection).

It should be pointed out that the value of the estimates obtained through the method above is relative only to the peculiar operative conditions in which they have been obtained. This means that a comparison with friction coefficient measurements obtained by classical and more precise methods would not make much sense in this context, and are therefore avoided here. Therefore, reference to "apparent" friction coefficients is meant in the above discussion. The point in estimating friction characteristics with the methods above described is that their results are repeatable in similar operative conditions.

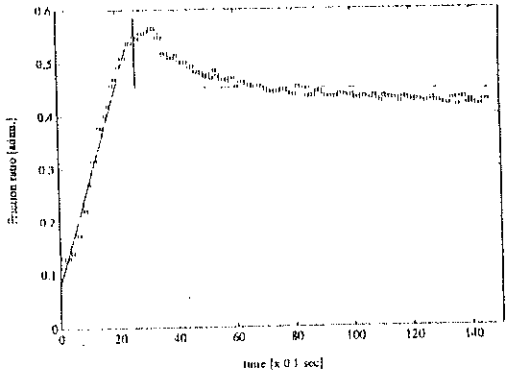

Figure 7: Friction ratio plot for an urethane steel pair

3.3 Rotational Friction Characteristics

Another series of experiments have been carried out in order to evaluate the feasibility of a direct measurement of rotational friction (pure torsion) coefficients, ν_s and ν_d. The procedure followed in this case is similar to the one for translational friction data, differing only for the means of obtaining a rotational slippage between the object and the finger (see Fig. 9).

Recalling equation 5, we observe that in this case the ratio to be monitored during the tests is

$$R_s = \frac{\eta_z}{(p_z)^{\frac{1}{3}}}.$$

Three typical plots of R_s vs. time are reported in Fig. 10 a), b), and c). These plots correspond to the same finger and object cover materials, but different values of the normal component of the contact force, p_z, which was controlled to a reference value of $12N$, $9N$, and $6N$, respectively. The static and kinetic rotational coefficients of friction are derived from raw measurements using the pattern-matching algorithm above illustrated: Fig. 10 shows the piecewise linear approximation superimposed to experimental data. For the three reported cases, the estimates of ν_s and ν_d are $\nu_s = 0.813\,N^{-1/3}mm$, $\nu_d = 0.686N^{-1/3}mm$, $\nu_s = 0.814\,N^{-1/3}mm$, $\nu_d = 0.737N^{-1/3}mm$, $\nu_s = 0.812\,N^{-1/3}mm$, $\nu_d = 0.792N^{-1/3}mm$, respectively. It can be seen from these results that the relationship 5 is in good agreement with experimental data. It must also be noted that the scattering of data about the expected pattern in rotational friction measurements is higher than for translational slip: this is caused by the lower signal-to-noise ratio in the measurement of rotational friction coefficients, which are inherently small for non-conformal contact surfaces.

3.4 Object Identification by Friction Characteristics

In order to assess the repeatability of friction characteristics evaluation by the methods above described, they have been repeatedly applied to a large set of objects, following the phases below:

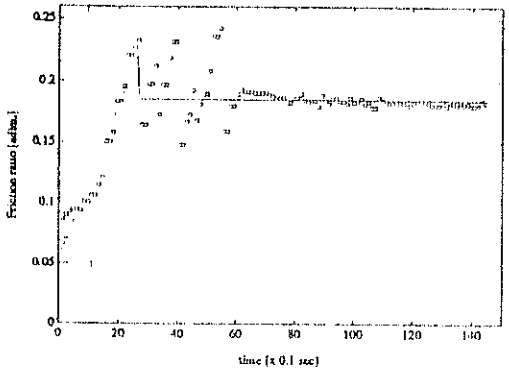

Figure 8: Friction ratio plot for a painted wood-steel pair

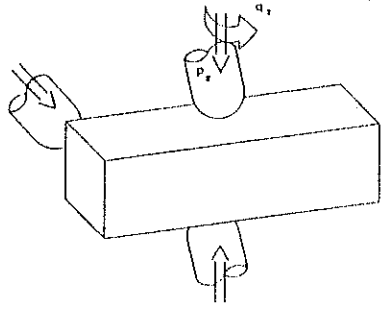

Figure 9: The experimental measurement of rotational friction limits

- objects of different shape and with different cover materials are collected in groups according to their superficial characteristics;
- the friction characteristics of an object out of each group are evaluated;
- the groups are merged into three classes, according to whether their kinetic translational friction coefficient is $\mu_d \leq 0.15$, $0.15 < \mu_d < 0.5$, $\mu_d \geq 0.5$;
- the objects are picked up by the robot hand at random, and are subject to friction measurement; based solely on friction data, the class of the objects are recognized.

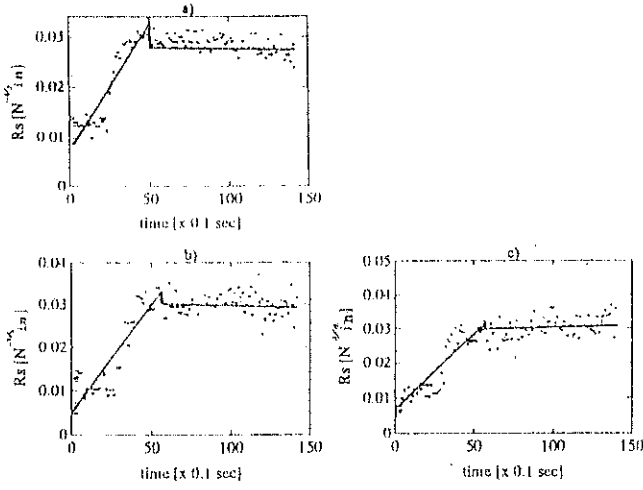

Figure 10: Rotational friction ratio plots for an urethane steel pair. a) $p_z = 12\ N$; b) $p_z = 9\ N$; c) $p_z = 6\ N$.

The groups of objects in the first class gather small ABS boxes and Teflon objects of different shapes. In the second class are collected wooden blocks with thickly painted surface; the third is comprised of objects with high friction surfaces (such as rubber toys and hoses). The experiment has been repeated more than 50 times over a two-months period, with full success.

4 Conclusions

Friction forces play a fundamental role in dexterous manipulation. When planning or executing an operations involving contacts with the environment or with manipulated objects, the knowledge of the limits of friction forces is instrumental to control (or simply avoid) slippage. Theoretical study of these limits shows that not only the effects of pure shear forces (as most often is held in robotics literature), but also those of torsions applied at the contact must be taken into account. This important fact has been noted in previous works ([12], [13], [15]), indicating that a good approximation of the friction limit curve can be obtained starting from limits in the pure shear and pure-torsion cases. In this paper, we presented results related to experimental measurements of such limits, that allow practical implementation of manipulative operations based on friction sensing, such as object recognition, adaptive grasping, controlled slippage, etc.

Acknowledgments

The authors would like to gratefully acknowledge the financial support from the following sources: the University Research Initiative Program under Office of Naval Research contract N00014-86-K-0685, NASA contract number NAG-9-319, and the Consiglio Nazionale delle Ricerche, Progetto Finalizzato Robotica. Support for Antonio Bicchi as a Visiting Scientist at the M.I.T Artificial Intelligence Laboratory has been granted through the NATO-CNR joint fellowship n.215.22/07.

References

[1] Mason, M.T. and Salisbury, J.K.: "Robot Hands and the Mechanics of Manipulation," MIT Press, Cambridge, MA, 1985.

[2] Jacobsen, S.C., Wood, J.E., Knutti, D.F., Biggers, K.B.: "The Utah-MIT Dextrous Hand: Work in Progress", in The Int. Jour. of Robotics Research, vol.3, no.4, pp. 21-50, 1984.

[3] Nicholls, H.R. and Lee, M.H.: "A Survey of Robot Tactile Sensing Technology," Int. Jour. of Robotics Research, Vol. 8, No .3, June 1989.

[4] Hackwood, S., Beni, G., Hornak, L.A., Wolfe, R., Nelson, T.J.: "Torque Sensitive Tactile Array for Robotics", in The Int. Jour. of Robotics Research vol.2, no. 2, 1983.

[5] Domenici, C., DeRossi, D., Bacci, A., Bennati, S.: "Shear Stress detection by a Piezoelectric Polymer Tactile Sensor", IEEE Trans. on Electr. Insulation, vol. EI 24, no.6, 1989.

[6] Bicchi, A., Salisbury, J.K., and Brock, D.L.: "Contact Sensing from Force Measurements", MIT AI Lab Memo no.1262, October 1990.

[7] Armstrong, B.: "Dynamics for Robot Control: Friction Modeling and ensuring excitation During Parameter Identification", Ph.D. Thesis, Electrical Engineering Dept., Stanford University, 1988.

[8] Armstrong-Helouvry, B.: "Stick-Slip Arising from Stribeck Friction", Proc. IEEE Int. Conf. on Robotics and Automation, 1990.

[9] Balestrino, A., and Bicchi, A.: "Adaptive Surface Following and Reconstruction Using Intrinsic Tactile Sensing," Proc. Int. Works. on Sensorial Integration for Industrial Robots, Zaragoza, Spain, 1989.

[10] Brock, D.L.: "Enhancing the dexterity of a Robot hand Using Controlled Slip", Proc. IEEE Int. conf. Robotics and Automation, 1988.

[11] Howe, R.D., and Cutkosky, M.R.: "Sensing Skin Acceleration for Slip and Texture Perception", Proc. IEEE Int. Conf. on Robotics and Automation, 1989.

[12] Jameson, J.W.: "Analythic Techniques for Automated Grasp", Doctoral Dissertation, Stanford University, 1985.

[13] Howe, R.D., Kao, I., and Cutkosky, M.R.: " The Sliding of Robot Fingers Under Combined Torsion and Shear Loading", Proc. IEEE Int. Conf. on Robotics and Automation, 1988.

[14] Goyal, S.: "Planar Sliding of a Rigid Body With Dry Friction: Limit Surfaces and Dynamics of motion", Ph.D. Thesis, Mech. Eng. Dept., Cornell University, Ithaca, 1989.

[15] Bicchi, A., Bergamasco, M., Dario, P., Fiorillo, A.S.: "Integrated Tactile Sensing for Gripper Fingers", Proc. Int. Conf. on Robot Vision and Sensory Control - RoViSeC '88, Zurich. I.F.S. Publications Ltd., 35-39 High Street, Kempston, Bedford MK 42 7BT, U.K., 1988.

[16] Salisbury, J.K., Brock, D.L., Chiu, S.L.: "Integrated Language, Sensing and Control for a Robot Hand", Proc. 3rd ISRR, Gouvieux, France, MIT Press, Cambridge MA, 1985.

[17] Chiu, S.L.: "Generating Compliant Motion of Objects with an Articulated Hand", M.S. Thesis, MIT AI Lab Technical Report 1029, 1985.

[18] Brock, D.L, and Chiu, S. "Environment Perceptions of an Articulated Robot Hand Using Contact Sensors," Proc. ASME Winter Annual Meeting, Miami, FL, 1985.

[19] Bicchi, A.: "On the Optimal Design of Multi Axis Force Sensors", MIT AI Lab Memo no.1263, October 1990.